IEEE Robotics and Automation Letters (RA-L) paper, presented at ICRA 2024, Yokohama, Japan. Cite as RA-L paper.

Shape-Conformable Suction Cups with Controllable Adaptive Suction on Complex Surfaces

Tianqi Yue, Hermes Bloomfield-Gadêlha and Jonathan Rossiter

***Abstract*—Suction is widely used in industry, but the adaptation of state-of-the-art suction cups on complex surfaces (i.e., curved, cornered, uneven, rough, etc.) are still limited. In this paper, we present a novel shape-conformable suction mechanism to achieve highly-adaptive suction on complex surfaces. The shape-conformable adaptive suction is obtained by squeezing a soft multi-layer structure on the substrate, to form a shape-to-roughness sealed suction region. Based on this mechanism, two shape-conformable suction cups (SCSCs) – a displacement-driven shape-conformable suction cup (S_{Disp}) and a force-driven shape-conformable suction cup (S_{Force}) – are designed. They both achieve highly-adaptive suction on challenging surface topographies including highly-curved, cornered, textured, uneven and tilted surfaces. Particularly, S_{Disp} has better adaptation (e.g., on a 90° corner and a balloon) and S_{Force} is more lightweight (26 g) and compact ($\varnothing 46 \times 35$ mm), and exhibits quicker suction response (0.4 s). We analyse the underlying adaptive suction mechanism by the physical model, and demonstrate its adaptive suction capability by qualitatively comparing it with previous suction cups. We finally conclude design principles for improving suction adaptation. We believe the proposed shape-conformable suction mechanism provides a novel solution to realize adaptive suction on complex surfaces in next-generation robotic gripping, anchoring and manipulation.**

I. Introduction

As a low-cost adhesion strategy, suction is one of the most popular methods used to carry large-size and heavy objects in industry [1]. High lifting ratio (object mass / gripper mass), low energy consumption, small contact area and switchable adhesion are the advantages of artificial suction cups compared to other adhesion methods [2]. However, suction is susceptible to surface complexity due to the leakage, e.g., curvature, roughness, etc., which makes the application of suction cups very limited on complex surfaces [2–6]. The industrial solution to this problem is applying a constant strong vacuum, but it is noisy, energy-wasting, and does not solve the underlying leakage problem [1]. A solution to reduce the suction leakage on complex surfaces would have great significance to the development of artificial suction cups.

TY was funded by Chinese Scholarship Council through award 201906120027. JR was supported through EPSRC research grants EP/V062158/1, EP/T020792/1, EP/V026518/1, EP/S026096/1 and EP/R02961X/1, and by the Royal Academy of Engineering as a Chair in Emerging Technologies.

Tianqi Yue, Hermes Bloomfield-Gadêlha and Jonathan Rossiter are with the Department of Engineering Mathematics and Bristol Robotics Laboratory at the University of Bristol, Bristol, BS8 1TW, UK. {tianqi.yue, hermes.gadelha, jonathan.rossiter}@bristol.ac.uk

Data are available at the University of Bristol data repository, data.bris, at https://doi.org/10.5523/bris.3d1sge14ol61b2tfr4xyc37xti

To achieve adaptive suction, the gap between the suction and the substrate must be small to reduce leakage. However, the surface complexity includes shapes and roughness. It is challenging for artificial suction cups to simultaneously conform to the shape and roughness of complex surfaces. Solutions for can be categorised into two categories. Jamming is a method used to conform to surface overall shape [7–10]. It realizes the shape conformation by the contact-induced deformations of an elastic bag filled with small granules, then it uses a vacuum pump to stiffen the bag and maintain the shape conformation. However, the stiffened bag lacks elasticity, therefore cannot passively generate the suction and needs an extra pump to maintain the suction pressure. Another method is fabricating suction cups with soft elastic materials, since soft materials can easily conform to surface small asperities by the squeezing pressure [11–16]. However, it cannot conform to surface shapes with large curvature. A comparison between a commercial suction cup, a jamming-based suction cup and a soft-material suction cup is shown in Fig.1. Our previous work proposed an adaptive soft suction cup but did not demonstrate very high adaptation on highly-curved or cornered surfaces [17]. Other methods for improving the adaptation include using stickiness [18] and multi-suction-cup arrays [19, 20]. In this work, we only focus on enhancing the adaptation of an individual suction cup, and do not consider the use of other bonding strategies.

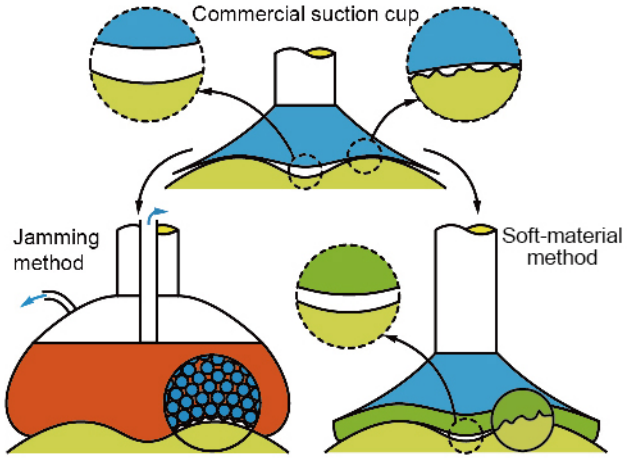

Fig. 1. The challenge of generating suction on complex surfaces. A commercial suction cup cannot conform to complex surface overall shapes nor roughness. A jamming-based suction cup lacks the conformation on surface roughness. A soft-material suction cup lacks the conformation on surface overall shapes.

In this paper, we present a new shape-conformable suction cup for achieving highly-adaptive suction on complex surfaces, including curved, cornered, tilted and rough surfaces, without constant air vacuuming. In Section.II, we present the mechanism of the shape-conformable suction achieved by squeezing a multi-layer structure composed of multiple materials with different properties. In Section.III, two shape-conformable suction cups with different actuation methods are designed and their fabrication methods are provided. In Section.IV, we demonstrate two suction cups' adaptation on challenging surfaces, which are highly-curved, cornered, uneven, deformable, rough and tilted. In Section.V, we discuss key factors that contribute to the adaptability of the shape-conformable suction based on its physical model. Finally, we conclude the contribution and future applications shape-conformable suction cups.

II. Shape-conformable Suction Mechanism

The shape-conformable suction mechanism achieved by the multi-layer structure is shown in Fig.2A. It has a similar structure as our previous work but with new designs of its actuation system which will be introduced later [17]. On the top there is a rigid constraining plate (1 in Fig.2A) used for squeezing the soft structures beneath it. Squeezing the thick layer of porous latex (2 in Fig.2A) makes the suction cup disc conform to the substrate shape. This shape conformation benefits from the open-cell porous structure of the porous latex (Fig.2B i), similar to previous cell-shaped adaptive grippers [21, 22] but with much smaller pore size and better adaptation on centimeter∼millimeter surface topographies. Beneath the porous latex there is a PVC suction cup (3 in Fig.2A) which acts as a skeleton to strengthen the whole suction cup structure. Bottom is a soft silicone pad (4 in Fig.2A) with low hardness (20 A) and Young's modulus (338 kPa), conforming to the smaller asperities by its elasticity. The three scenarios shown in Fig.2B demonstrate the shape-conformable suction on a curved and rough surface. The porous latex conforms to the surface's overall shape well, but it cannot generate suction due to the air leakage through pores (Fig.2B i). The whole structure is strengthened after adding the PVC suction cup but air still could leak from the small apertures (Fig.2B ii). Adding the

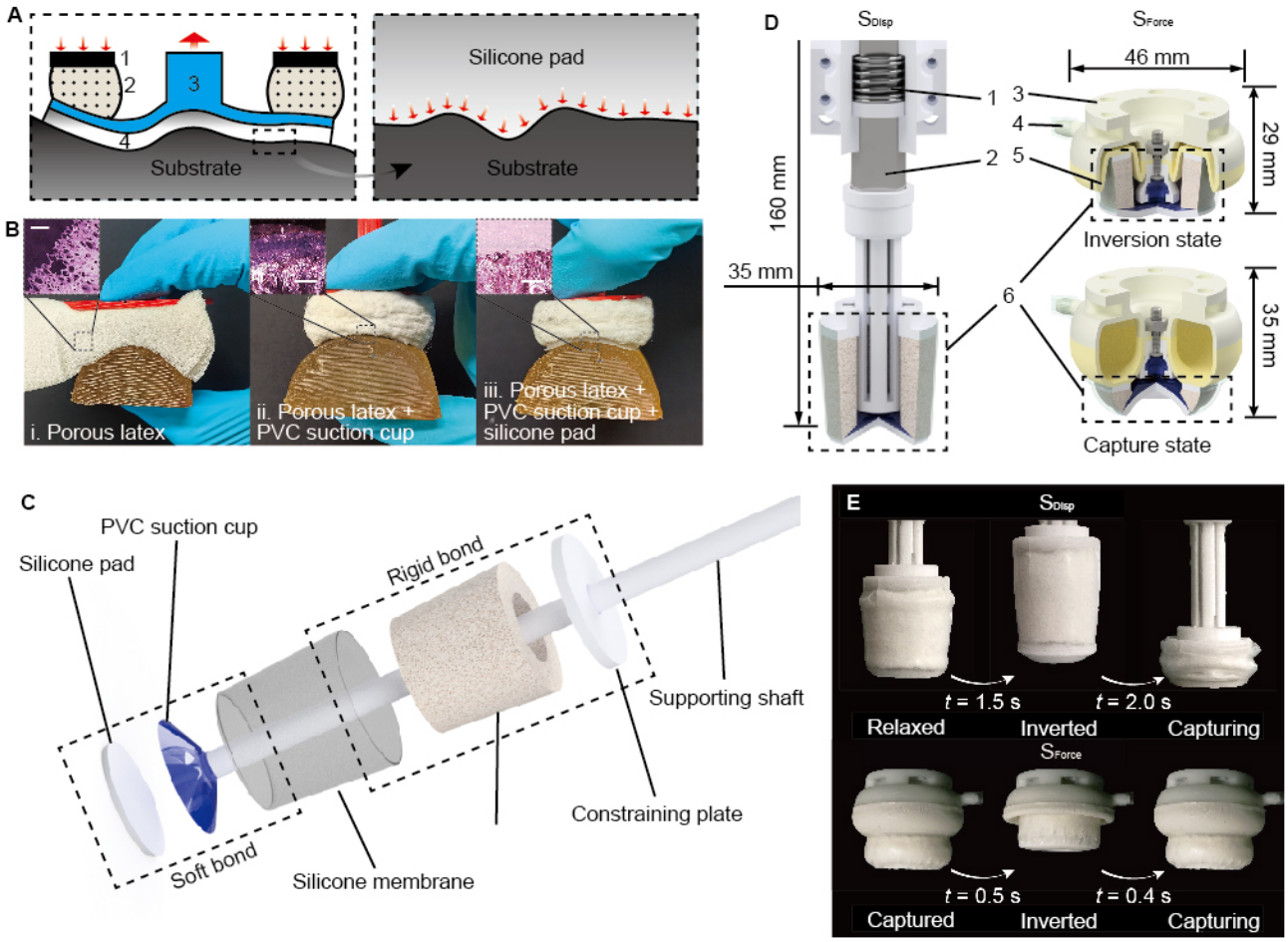

Fig. 2. The diagram and working principle of shape-conformable suction cups. (A) The shape-conformable suction mechanism. 1: constraining plate. 2: porous latex. 3: PVC suction cup skeleton. 4: silicone pad. (B) The establishment of the shape-conformable suction on a curved and rough surface. Inserts: microscopic photos at the contact interface. Scale bars: 500 μm. (C) The structure of the shape-conformable suction part. (D) Structures of S_{Disp} and S_{Force}. 1: mitigating spring. 2: linear actuator. 3: lid. 4: air inlet/outlet. 5: snaping membrane. 6: suction part (same as (C)). (E) Actuation difference between S_{Disp} and S_{Force}.

IEEE Robotics and Automation Letters (RA-L) paper, presented at ICRA 2024, Yokohama, Japan. Cite as RA-L paper.

soft silicone pad finally reduces apertures to a small enough scale such that adaptive suction can be established (Fig.2B iii). In summary, squeezing the multi-layer structure, a composite of different material properties, can successfully form an adaptive suction region on complex surfaces from overall shape to roughness. Detailed designs will be illustrated later.

III. Design of Shape-conformable Suction Cups

Apart from the adaptability, a suction cup needs both the attachment (to capture) and detachment (to release) functionalities. Fig.2C shows the structure for achieving the transition between the two states. A cylindrical silicone membrane (0.5 mm thickness, 60 A hardness, LMS) bonds the rim of the silicone pad and the constraining plate at its two ends. Therefore, pushing the constraining plate squeezes the multi-layer structure to generate the suction, and pulling the constraining plate can lift the suction cup rim by transmitting tension through the cylindrical silicone membrane to break the suction. The silicone pad, PVC suction cup and silicone membrane are bonded by silicone glue (X-1910, Setllom) to ensure compliance, while the silicone membrane, porous latex and constraining plate are bonded by instant glue (A-400, Kooton).

Two shape-conformable suction cups (SCSCs) shown in Fig.2D have the same sucker structure (Fig.2C). The difference between the two SCSCs is only the actuation method. One suction cup is actuated by a linear actuator (L13060202106-1, Taihengli), which can travel up to 50 mm and provide up to 60 N squeezing force. The pusher of the linear actuator can be controlled to stop at the required position, therefore it is named the "displacement-driven" suction cup (S_{Disp}). Another one is actuated by a pneumatic soft toroidal-shaped snaping membrane, which always provides an approximately constant squeezing force $\sim$40 N, therefore it is named the "force-driven" suction cup (S_{Force}). S_{Force} can only switch between the inversion state (backward snaping) and capture state (forward snaping) due to the binary snaping property, as Fig.2D shows. However, S_{Force} exhibits a quicker response ($\sim$0.4 s) than S_{Disp} thanks to the snaping property.

The fabrication of the two suction cups is as follows. Rigid parts are FDM-3D-printed by PLA. The linear actuator of S_{Disp} is mitigated by a compression spring with stiffness of 30.67 N/mm. The snaping membrane of the S_{Force} is fabricated by casting urethane rubbers (VytaFlex 60, Smooth on). The porous latex is cut from a piece of commercial porous latex sheet with size of $\varnothing 20 \times \varnothing 34 \times 30$ mm (inner diameter $\times$ outer diameter $\times$ thickness). The silicone pad is made by casting silicone (Dragon Skin 20, Smooth-on) with the dimension of $\varnothing 30 \times 2$ mm. Two suction cups are with the same diameter ($\varnothing 30$ mm), the total mass of the S_{Disp} and S_{Force} are 100 g and 26 g (syringe not included), respectively.

We use Fig.3 to show a grip-manipulate-release cycle of S_{Force} gripping a heavy and highly-curved bottle (529.5 g). S_{Disp} has a similar working mode which can be seen in Movie.S1. Initially, S_{Force} is relaxed. When S_{Force} is about to grip the object, the syringe vacuums to invert the snaping membrane, thereby S_{Force} is at the inverted state. In this state, the centre of the suction cup bottom is outermost. The user or robot moves the suction cup to contact with the object. Then the syringe pumps air in to let the snaping membrane snap forward to squeeze the multi-layer structure, therefore S_{Force} conforms to the object surface and the shape-conformable suction is generated. The object can then be picked up and manipulated. To release, the syringe pumps air out again to make the snaping membrane re-invert by lifting the suction cup rim, therefore the suction is eliminated. Finally, the syringe pumps air in again to reset S_{Force} to its relaxed state.

IV. Adaptive Suction Performance Evaluation

Videos of evaluating the suction adaptation can be seen in Movie.S1. First, we evaluate the adaptability on complex surface shapes. Three types of quadric surfaces – the ellipsoids (EP, convex both on x axis and y axis), hyperbolic paraboloids (HP, convex on x axis and concave on y axis) and parabolic cylinders (PC, convex on x axis and flat on y axis), were prepared to represent most curved surfaces in real world. These surfaces are parameterized as shown in Tab.I. In addition, a flat plate was also prepared for comparison. All samples were SLA-3D-printed by resin, and polished by sandpapers (EAGLE&AX SILICIUMCARBID) to ensure smoothness. This is to ensure that only one variable is varied in order to test shape adaptation.

TABLE I
Quadric Surfaces Parameters

Name	Equation	a	b	c
EP_1 to EP_5	$\frac{x^2}{a^2}+\frac{y^2}{b^2}+\frac{z^2}{c^2}=1$	5, 10, 15, 20, 25	$=2a$	$=a$
HP_1 to HP_5	$\frac{x^2}{a^2}-\frac{y^2}{b^2}+z=0$	4, 5, 6, 7, 8	$=2a$	N/A
PC_1 to PC_5	$x^2+2az=0$	5, 10, 15, 20, 25	N/A	N/A

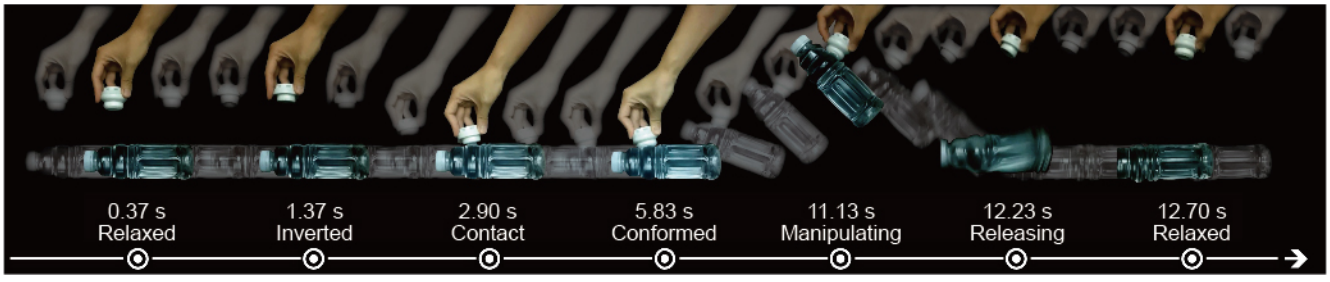

Fig. 3. Time-lapse of S_{Force} gripping a highly-curved and heavy bottle filled with water (529.5 g).

The first property to be characterized is the maximum suction force F_{s_max}. To measure it, the suction cup was carried by a linear stage to move down and up until the suction cup broke off from the substrate. Prepared quadric samples were fixed on a load cell (SB, Maxwell Measurement) for measuring the force at the suction interface. For S_{Disp}, the linear actuator was always set to squeeze the multi-layer structure to the pushing limit (50 mm) unless it reaches the force limit (60 N). For S_{Force}, a syringe was used to drive the snaping membrane. A pressure sensor (HHP50-03, HHCON) was connected for monitoring the relative pressure differential between the snaping chamber and the atmosphere. Measured transitioning pressure differential are -23 kPa (inversion-capture transition) and -33.6 kPa (capture-inversion transition). F_{s_max} is the measured force at the breaking-off moment when the linear stage is slowly ($\sim$3.125 mm/s) pulling the suction cup away from the sample surface. A $\varnothing$30 mm PVC suction cup (S_{PVC}, same as the one used in Fig.2C), was also tested for comparison. Four force-time graphs during the measurement on different samples show the loading-unloading process (Fig.4A-B). Note that the linear stage must exert a preload ($\sim$ 5 N based on our experience) to let the suction cup make solid contact with the sample against the following squeezing force from the actuator. The maximum suction force was recorded at the breaking moment.

All samples were tested 10 times to ensure reliability. Measured F_{s_max} on EP, HP and PC are shown in Fig.4D-F. The scenarios of shape conformation of S_{Disp}, S_{Force} and S_{PVC} on EP_4/HP_4/PC_4 samples are shown in Fig.4C. Gaps are observed in S_{PVC} photos – showing insufficient adaptation to form the suction, while S_{Disp} and S_{Force} show good conformation to the sample shape. With the curvature increasing, S_{PVC} sharply loses suction while S_{Disp} and S_{Force} still can generate non-zero suction force, until the surface curvature becomes too large (EP_1/HP_1/PC_1). This demonstrates the adaptive suction of S_{Disp} and S_{Force}. In addition, S_{Disp} has better adaptation than S_{Force} especially on highly-curved samples (e.g., EP_2). However, the maximum suction force of S_{Disp} and S_{Force} measured on the flat surface (dashed lines) are slightly smaller than S_{PVC}. We will discuss the experimental results later.

Three suction cups were then tested to grip spheres, cylinders and corners to evaluate their adaptation on these most common shapes. Gripping the object and maintaining the suction for 1 minute is defined as a success, and each sample was tested 10 times. Spheres with diameters from $\varnothing$10 mm to $\varnothing$20 mm and cylinders with diameters from $\varnothing$10 mm to $\varnothing$30 mm were used for testing. Corners are divided into two groups. A challenging group with 90° angle was fabricated with fillet radii of 0, 0.5, 1, 3 and 5 mm, for testing S_{Disp}. An easier group is with angle of 110°, 115°, 120°, 140° and 160°, for testing S_{Force}, since S_{Force} is not able to grip the 90° corner sample. All the samples were SLA-3D-printed with resin and polished.

Fig.5A-F show the experimental results of gripping these objects. S_{PVC} cannot grip any of these objects, and S_{Disp} still performs better than S_{Force}. S_{Disp} reaches 100% gripping success rate on all the spheres (Fig.5A) and is able to grip cylinders as small as $\varnothing$16 mm (Fig.5B). The S_{Force} is able to pick up spheres with 100% gripping success rate as small as $\varnothing$18 mm and cylinders as $\varnothing$26 mm. Photos in Fig.5C show the conformation of three suction cups on these samples. Adaptation differences between S_{Disp} and S_{Force} is more distinct on corner samples.

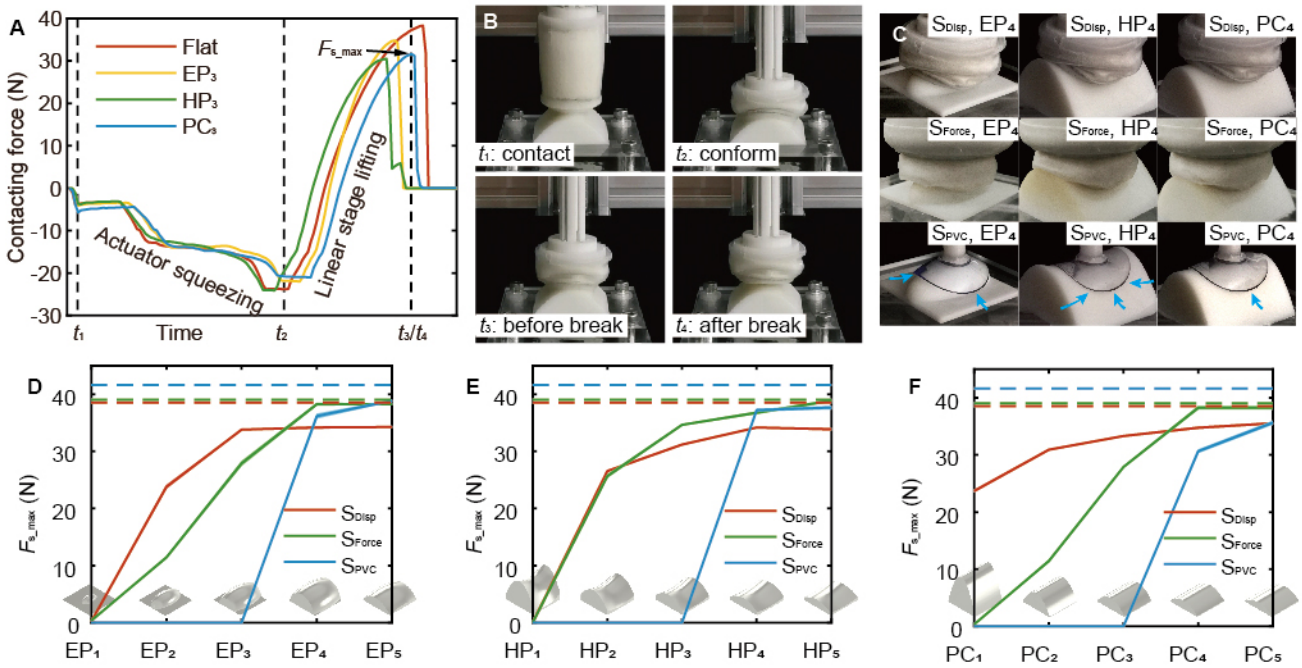

Fig. 4. Maximum suction force measured on quadric surfaces. (A) Contacting force-time graphs on four samples with different shapes. (B) Scenarios of four key moments during the PC_3 test, corresponding to (A). (C) Photos show the shape conformation scenarios of S_{Disp}, S_{Force} and S_{PVC} on EP_4/HP_4/PC_4 samples. (D) F_{s_max} measured on EP samples. (E) F_{s_max} measured on HP samples. (F) F_{s_max} measured on PC samples.

IEEE Robotics and Automation Letters (RA-L) paper, presented at ICRA 2024, Yokohama, Japan. Cite as RA-L paper.

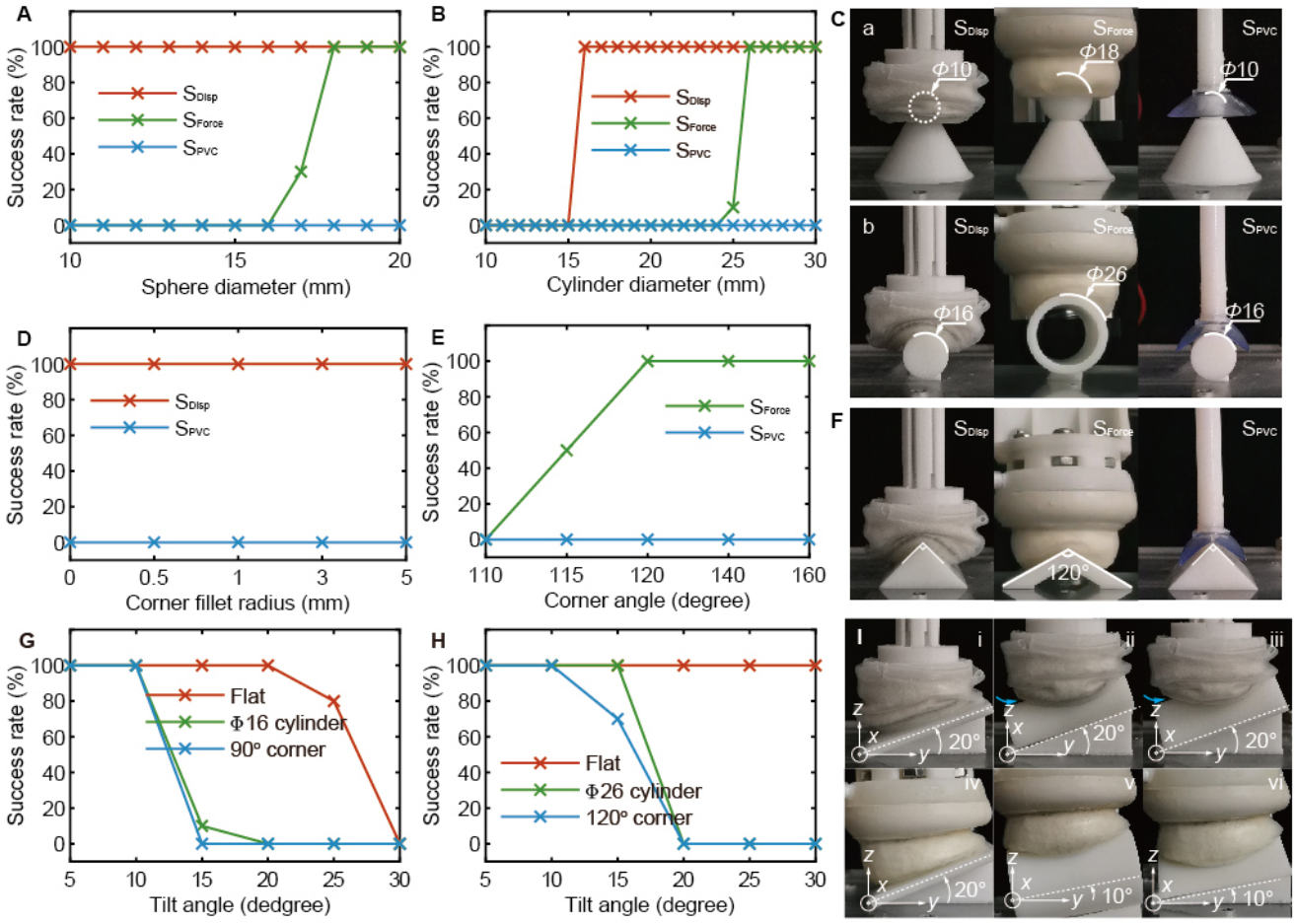

Fig. 5. Gripping test on spheres, cylinders and corners. (A) Success rate on spheres. (B) Success rate on cylinders. (C) Conformation scenarios of S_{Disp}, S_{Force} and S_{PVC} on spheres and cylinders. (D) Success rate of S_{Disp} on 90° corners with different fillets. (E) Success rate of S_{Force} on corners with different angles. (F) Conformation scenarios of S_{Disp}, S_{Force} and S_{PVC} on tested corner samples. (G) Success rate of S_{Disp} on tilted flat plate, ⌀16 mm cylinder and 90° corner (0 mm fillet). (H) Success rate of S_{Force} on tilted flat plate, ⌀26 mm cylinder and 120° corner. (I) Shape conformation scenarios of S_{Disp} on tilted flat plate (i), ⌀16 mm cylinder (ii) and 90° corner (iii), S_{Force} on tilted flat plate (iv), ⌀26 mm cylinder (v) and 120° corner (vi).

S_{Disp} is able to grip all the 90° corner samples with 100% success rate as shown in Fig.5D, even with 0 mm fillet. S_{Force} cannot pick up any 90° corner sample and is able to grip corners as small as 120° as shown in Fig.5E. The shape conformation scenarios are shown in Fig.5F.

Three suction cups were tested to pick up tilted objects which are common situations in real robotic applications, since the axis of the suction cup is not always perpendicular to the object's surface. Based on the former results, we set two groups of samples for testing. For S_{Disp}, a flat plate, a ⌀16 mm cylinder and a 90° corner (0 mm fillet radius) were used. For S_{Force}, a flat plate, a ⌀26 mm cylinder and a 120° corner were used. These samples were placed on a tilted bracket as shown in Fig.5I. Each sample was tested 10 times and the success is also defined as maintaining the suction for 1 minute. As shown in Fig.5G, S_{Disp} successfully grips the flat plate with tilt angle $\leq$25°. For ⌀16 mm cylinder and 90° corner, S_{Disp} only succeeds when the tilt angle $\leq$10°. According to Fig.5H, S_{Force} grips the flat plate with tilt angle up to 30°, the ⌀26 mm cylinder with tilt angle $\leq$15° and the 120° corner with tilt angle $\leq$10°. Both the two shape-conformable suction cups show tolerance on tilted objects, while S_{Force} is slightly better due to the inherent softness of the snaping membrane, which distributes the squeezing stress to the multi-layer structure more evenly than the linear actuator. This can be seen through the deformed shape of the snaping membrane as shown in Fig.5I. Overall, the experimental results reveal that S_{Disp} and S_{Force} do not require precise position control in practical applications.

To demonstrate the influence of the silicone pad's Young's modulus on the roughness adaptation, we fabricated another suction cup, S_{Force_hard}, with a harder silicone pad (Dragon Skin 30, Smooth-on) with Young's modulus of 593 kPa and hardness of 30 A. Rest components of S_{Force_hard} are same as S_{Force}, which is with the softer silicone pad (338 kPa, 20 A). Four surface samples were prepared for the test: a smooth flat sample, a rough (180 grit) flat sample, a smooth ⌀30 cylinder sample and a rough (180 grit) ⌀30 cylinder sample. Each sample was tested to grip ten times by the two suction cups. Results shown in Fig.6 demonstrate that both S_{Force} and S_{Force_hard} are able to grip the two smooth samples, while only the S_{Force} (with softer

IEEE Robotics and Automation Letters (RA-L) paper, presented at ICRA 2024, Yokohama, Japan. Cite as RA-L paper.

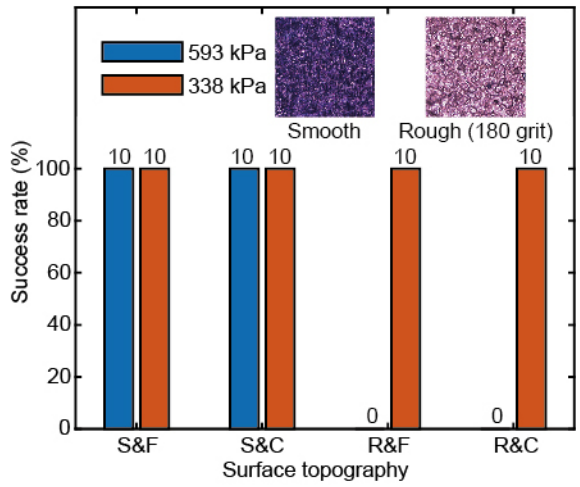

Fig. 6. Comparison between S_{Force} (338 kPa) and S_{Force_hard} (593 kPa) with different silicone pad hardness. F: flat. C: ⌀30 cylinder. S: smooth. R: rough (180 grit). Numbers above bars are the number of successful grips, out of 10 trials.

silicone pad)) successfully gripped the rough samples.

Finally, S_{Disp} and S_{Force} were used to grip a variety of real-world objects. 16 objects with different complex surface topographies were selected to do the test as shown in Fig.7. S_{Disp} and S_{Force} both succeed to grip objects with high irregularities, such as a heavy water bottle (Fig.7A/B (i)), tubes (Fig.7A/B (j) and (k)) and textured surfaces (Fig.7A/B (l)). Note that, we did not let S_{Disp} squeeze the multi-layer structure with its highest output force (60 N). We adjusted the squeezing distance according to the object property to obtain better suction performance. For example, a short squeezing distance was used to grip a lamp, which is heavy but less curved (Fig.7A (o)). A short squeezing distance was also used to grip deformable objects such as a balloon (Fig.7A (p)), to avoid damaging it. A large squeezing distance was used for gripping highly-curved objects, e.g., the bottle (Fig.7A/B (i)). We will explain the reason for this manner later. Due to the snaping property of bifurcation, S_{Force} cannot control the squeezing distance of the multi-layer structure, therefore it cannot grip super-soft objects such as the balloon, but still succeeds on stiffer objects such as a pork belly (Fig.7B (p)). To sum up, both S_{Disp} and S_{Force} show quite good adaptive suction performance on most of the complex-shaped real-world objects, while S_{Disp} has better adaptation due to its controllable squeezing distance. Videos of gripping real-world objects can be seen in Movie.S2.

V. Discussion

A. Physical Model, Maximum Suction Force and Adaptation

Although the structure of shape-conformable suction cups involves multiple soft materials with different properties and high non-linearity, the following physical model can be used to approximately predict suction force and shows good agreement with our experimental results:

$$\begin{aligned} F_{s\_max} &= \Delta p A_{proj} - F_{deform}, \\ F_{deform} &= 0.0052 d_s^3 - 0.13 d_s^2 + 1.1 d_s + 4.71. \end{aligned} \quad (1)$$

where Δp is the pressure differential between the atmospheric pressure and the internal suction pressure, A_{proj} is the area projection on the suction cup normal direction, F_{deform} is the measured deformation-induced force (i.e., the squeezing of the porous latex and bending of the PVC suction cup), d_s (mm) is the squeezing distance of the porous latex layer. Based on Eq.(1), increasing F_{deform} (i.e., squeezing more on the porous latex) will reduce the maximum suction force F_{s_max}. This is consistent with the trend of experimental results shown in Fig.4. On flat surface, measured F_{s_max} of $S_{PVC}(41.64\ N) > S_{Force}(39.05\ N) > S_{Disp}(38.54\ N)$, since the F_{deform} of $S_{Disp}(60\ N) > S_{Force}(40\ N) > S_{PVC}(5\ N)$. It is worth noting that Eq.(1) is a simplified static force balance model at the suction interface. To predict the accurate suction force, complex conditions (e.g., the contact and friction mechanics, the surface topographies, etc.) must be considered. However, they are not the focus of this work.

The shape adaptation of three suction cups shows the opposite relation to their maximum suction force, i.e., S_{Disp} is slightly better than S_{Force} and they are both much better than S_{PVC}. This is demonstrated by the experimental results on non-flat surfaces shown in Fig.4, Fig.5 and Fig.7. This indicates that the maximum suction force and the shape adaptation of presented shape-conformable suction cups is a trade-off.

Experimental results shown in Fig.6 demonstrate that the silicone pad with lower Young's modulus helps the suction cup adapt to rough surfaces. This is consistent with the expected roughness adaptation, which can be explained by the contact mechanics at the suction interface [23]. Details of the micro-scale contact mechanics reported in Ref.[23] are quite complex, but we can discuss the parameters and relations we are interested. [23] indicates that the gap size u between two contacting surfaces is positively correlated with the Young's modulus E_1 of the suction bottom material and the Young's modulus E_2 of the substrate, i.e., $u \propto E_1,\ E_2$. Larger u causes faster leakage, which makes the suction quality worse. Therefore, lower E_1 and E_2 allow for a better suction on rough surfaces. However, substrate Young's modulus E_2 cannot be determined by the suction cup design. Therefore, suction cup bottom materials' Young's modulus E_1 is the only customisable parameter. In summary, softer suction cup bottom material can reduce the gap between the suction cup and small asperities on the substrate, which explains why S_{Force} demonstrates better adaptation than S_{Force_hard} on rough surfaces.

B. Gripping Strategy

Given the discussion on the maximum suction force and suction adaptation above, we provide a qualitative gripping strategy for achieving appropriate adaptive suction on various objects. Less-curved and heavy objects (e.g., Fig.7A (o)) require higher adhesive force, therefore a smaller squeezing distance (5∼10 mm) is sufficient to form the suction region and generate a high suction force. In contrast, highly-curved and rough objects (e.g., Fig.7A (i)) require a larger squeezing distance (>10 mm) to allow for better shape conformation. Note that the controllable squeezing distance is only applicable for S_{Disp}.

Fig. 7. Demonstration of shape-conformable suction cups picking up a variety of real-world objects. (A) Picking-up scenarios of S_{Disp}. (d), (e), (i) and (m) are with large curvature, (i), (n) and (o) are heavy, (j) and (k) are uneven, (l) has textures, (n) has corners, (k) and (p) are deformable. (B) Picking-up scenarios of S_{Force}. (d), (e), (g), (i), and (m) are with large curvature, (i), (m) and (n) are heavy, (j) and (k) are uneven, (l) has textures, (f) and (n) have corners, (k) and (p) are deformable.

C. Qualitative Comparison

As demonstrated above, both shape-conformable suction cups obtained high suction force and adaptation on complex surfaces. We collect data of S_{Disp}, S_{Force} and previous adaptive suction cups in Tab.II and make a qualitative comparison of their adaptability [7, 11–13, 15, 16, 18, 24]. Three parameters, $\eta_{\text{suction}}(1) = 4F_{\text{s\_max}}/(\pi d^2 p_{\text{atm}})$, $\eta_{\text{mass}}(1) = F_{\text{s\_max}}/(mg)$ and $\eta_{\text{size}}(\text{N/cm}) = F_{\text{s\_max}}/l_{\text{max}}$, are defined for describing their suction performance. d (mm) is the suction cup diameter, m (kg) is the suction cup mass and l_{max} (cm) is the maximum dimension of the gripper. They are the ratio of the measured maximum suction force and the theoretical maximum suction force, the suction gripper mass and the maximum gripper dimension, respectively represent the suction power density, the lifting efficiency and the gripper compactness. Tab.II indicates that shape-conformable suction cups are with relatively high suction power density compared to others. In addition, S_{Disp} exhibits the highest adaptation except for grooved surfaces and S_{Force} has relatively light weight and compact size. It is worth noting that all the adaptive suction cups have their own unique features, and we only focus on their suction adaptability and make a qualitative comparison in this paper.

VI. Conclusions

In this paper, we presented a novel shape-conformable suction mechanism for achieving highly-adaptive suction on complex surfaces. In contrast to conventional suction cups, the proposed shape-conformable suction cups do not need a vacuum pump to constantly pump air out in order to maintain suction on complex surfaces. Therefore, they are more energy-efficient and only consume energy during the state transition. The shape-conformable suction is realized by squeezing a multi-layer structure, which is composed of a porous latex, a suction cup skeleton and a silicone pad, onto a surface to form a shape conformation. The sealed suction region significantly reduces air leakage and it thereby generates strong adaptive suction force without active vacuuming. Two shape-conformable suction cups were designed and both achieved adaptive suction on complex surfaces, including quite small spheres, cylinders, sharp corners and a variety of challenging real-world objects. Both the proposed suction cups demonstrated gripping tolerance on tilted objects, reducing the requirement of control precision in future applications. Comparing the two suction cups, we demonstrated that the shape adaptation of the suction cup and its maximum suction force is a trade-off, which can be controlled by adjusting the squeezing force/distance on the multi-layer structure. In addition, we demonstrated the important influence of Young's modulus on roughness adaptation, where a lower Young's modulus for the suction cup surface material leads to better adaptive suction on rough surfaces.

Future work will focus on improving the suction adaptability further. First, the overall shape conformation is a trade-off between the material's Young's modulus, porosity and pore size, etc. Therefore, porous materials with customisable properties, such as silicone sponges, could be a better choice than porous latex. Second, liquid-enhanced suction, e.g., applying water or silicon oil to the suction interface, can combine with the shape-conformable suction structure to further improve the suction

TABLE II
COMPARISON OF ADAPTIVE SUCTION CUPS[1].

Ref.	d	F_{s_max}[2]	$\eta_{suction}$	η_{mass}[3]	η_{size}	Feature	Surface complexity					
							Curved	Uneven	Rough	Deformable	Grooved	Cornered
[7]	60	46	0.16	N/A	7.67	Enhanced by liquid	●	●	◐	N/A	●	◐
[11]	60	12	0.04	1.2	0.37	Soft contact	●	N/A	N/A	N/A	N/A	●
[24]	41	5.2	0.04	50	1.93	Origami structure[4]	●	N/A	N/A	N/A	N/A	●
[12]	25	7	0.14	311	2.8	Underwater applications	◐	●	●	N/A	N/A	N/A
[13]	18	7.7	0.30	476	4.28	High lifting ratio	◐	N/A	●	●	N/A	N/A
[15]	20	7.4	0.23	N/A	N/A	Grip small objects	◐	N/A	◐	◐	N/A	N/A
[16]	32	29	0.36	N/A	9.67	Adaptation on roughness	◐	N/A	●	◐	N/A	N/A
[17]	30	15.1	0.21	N/A	3.36	Contact-triggered capture	●	N/A	◐	N/A	N/A	N/A
S_{Disp}	**30**	**39.7**	**0.55**	**40**	**2.48**	**Higher adaptiation**	●	●	◐	●	○	●
S_{Force}	**30**	**38.5**	**0.54**	**148**	**8.37**	**lightweight and compact**	●	●	◐	◐	○	◐

[1] Adaptive suction cups combined with other adhesion strategies are not included, such as [18] using stickiness, [25] using electro-adhesion, etc.
[2] Measured F_{s_max} depends very much on the shape of surface. We cite the maximum forces reported in the references.
[3] For [7, 13, 18, 24] and S_{Force}, the mass of air pump is not included.
[4] This has a vacuum system to constantly pump air out.

adaptation on rough surfaces. Furthermore, the force-driven suction cup can be readily embedded into a multi-suction-cup system thanks to its facile actuation method and compact size. In summary, we believe that this work on adaptive suction cups provides a new path to develop highly-adaptive, energy-efficient, lightweight and compact suction cups for next-generation robotics, and provides the design principles for future adaptive suction cups.

REFERENCES

[1] Piab, "Suction cups for industry," https://www.piab.com/suction-cups-and-soft-grippers/ Accessed June 05, 2023.

[2] J. Shintake, V. Cacucciolo, D. Floreano, and H. Shea, "Soft robotic grippers," *Advanced Materials*, vol. 30, no. 29, p. 1707035, 2018.

[3] H. Bing-Shan, W. Li-Wen, F. Zhuang, and Z. Yan-zheng, "Bio-inspired miniature suction cups actuated by shape memory alloy," *International Journal of Advanced Robotic Systems*, vol. 6, no. 3, p. 29, 2009.

[4] N. Sholl, A. Moss, W. M. Kier, and K. Mohseni, "A soft end effector inspired by cephalopod suckers and augmented by a dielectric elastomer actuator," *Soft robotics*, vol. 6, no. 3, pp. 356–367, 2019.

[5] F. Tramacere, M. Follador, N. Pugno, and B. Mazzolai, "Octopus-like suction cups: from natural to artificial solutions," *Bioinspiration & biomimetics*, vol. 10, no. 3, p. 035004, 2015.

[6] S. Wang, L. Li, W. Sun, D. Wainwright, H. Wang, W. Zhao, B. Chen, Y. Chen, and L. Wen, "Detachment of the remora suckerfish disc: kinematics and a bio-inspired robotic model," *Bioinspiration & Biomimetics*, vol. 15, no. 5, p. 056018, 2020.

[7] T. Tomokazu, S. Kikuchi, M. Suzuki, and S. Aoyagi, "Vacuum gripper imitated octopus sucker-effect of liquid membrane for absorption," in *2015 IEEE/RSJ International Conference on Intelligent Robots and Systems (IROS)*. IEEE, 2015, pp. 2929–2936.

[8] T. Takahashi, M. Suzuki, and S. Aoyagi, "Octopus bioinspired vacuum gripper with micro bumps," in *2016 IEEE 11th Annual International Conference on Nano/Micro Engineered and Molecular Systems (NEMS)*. IEEE, 2016, pp. 508–511.

[9] M. Fujita, S. Ikeda, T. Fujimoto, T. Shimizu, S. Ikemoto, and T. Miyamoto, "Development of universal vacuum gripper for wall-climbing robot," *Advanced Robotics*, vol. 32, no. 6, pp. 283–296, 2018.

[10] K. Gilday, J. Lilley, and F. Iida, "Suction cup based on particle jamming and its performance comparison in various fruit handling tasks," in *2020 IEEE/ASME International Conference on Advanced Intelligent Mechatronics (AIM)*. IEEE, 2020, pp. 607–612.

[11] J. M. Krahn, F. Fabbro, and C. Menon, "A soft-touch gripper for grasping delicate objects," *IEEE/ASME Transactions on Mechatronics*, vol. 22, no. 3, pp. 1276–1286, 2017.

[12] J. A. Sandoval, S. Jadhav, H. Quan, D. D. Deheyn, and M. T. Tolley, "Reversible adhesion to rough surfaces both in and out of water, inspired by the clingfish suction disc," *Bioinspiration & biomimetics*, vol. 14, no. 6, p. 066016, 2019.

[13] S. Song, D.-M. Drotlef, D. Son, A. Koivikko, and M. Sitti, "Adaptive self-sealing suction-based soft robotic gripper," *Advanced Science*, p. 2100641, 2021.

[14] S. Song, D.-M. Drotlef, C. Majidi, and M. Sitti, "Controllable load sharing for soft adhesive interfaces on three-dimensional surfaces," *Proceedings of the National Academy of Sciences*, vol. 114, no. 22, pp. E4344–E4353, 2017.

[15] A. Koivikko, D.-M. Drotlef, C. B. Dayan, V. Sariola, and M. Sitti, "3d-printed pneumatically controlled soft suction cups for gripping fragile, small, and rough objects," *Advanced Intelligent Systems*, vol. 3, no. 9, p. 2100034, 2021.

[16] G. W. Hwang, H. J. Lee, D. W. Kim, T.-H. Yang, and C. Pang, "Soft microdenticles on artificial octopus sucker enable extraordinary adaptability and wet adhesion on diverse nonflat surfaces," *Advanced Science*, p. 2202978, 2022.

[17] T. Yue, W. Si, A. J. Partridge, C. Yang, A. T. Conn, H. Bloomfield-Gadêlha, and J. Rossiter, "A contact-triggered adaptive soft suction cup," *IEEE Robotics and Automation Letters*, vol. 7, no. 2, pp. 3600–3607, 2022.

[18] H. Tsukagoshi and Y. Osada, "Soft hybrid suction cup capable of sticking to various objects and environments," in *Actuators*, vol. 10, no. 3. Multidisciplinary Digital Publishing Institute, 2021, p. 50.

[19] R. Chen, L. Wu, Y. Sun, J.-Q. Chen, and J.-L. Guo, "Variable stiffness soft pneumatic grippers augmented with active vacuum adhesion," *Smart Materials and Structures*, vol. 29, no. 10, p. 105028, 2020.

[20] T.-V. Nguyen and I. Shimoyama, "Micrometer-sized suction cup array with strong adhesion to wet surface," in *2019 20th International Conference on Solid-State Sensors, Actuators and Microsystems & Eurosensors XXXIII (TRANSDUCERS & EUROSENSORS XXXIII)*. IEEE, 2019, pp. 1643–1646.

[21] J. Lee, Y.-S. Seo, C. Park, J.-s. Koh, U. Kim, J. Park, H. Rodrigue, B. Kim, and S.-H. Song, "Shape-adaptive universal soft parallel gripper for delicate grasping using a stiffness-variable composite structure," *IEEE Transactions on Industrial Electronics*, 2020.

[22] Y.-S. Seo, J.-Y. Lee, C. Park, J. Park, B.-K. Han, J.-S. Koh, U. Kim, H. Rodrigue, J. Bak, and S.-H. Song, "Highly shape-adaptable honeycomb gripper using orthotropic surface tension," *IEEE Transactions on Industrial Electronics*, 2023.

[23] C. Yang and B. Persson, "Contact mechanics: contact area and interfacial separation from small contact to full contact," *Journal of Physics: Condensed Matter*, vol. 20, no. 21, p. 215214, 2008.

[24] Z. Zhakypov, F. Heremans, A. Billard, and J. Paik, "An origami-inspired reconfigurable suction gripper for picking objects with variable shape and size," *IEEE Robotics and Automation Letters*, vol. 3, no. 4, pp. 2894–2901, 2018.

[25] Y. Okuno, H. Shigemune, Y. Kuwajima, and S. Maeda, "Stretchable suction cup with electroadhesion," *Advanced Materials Technologies*, vol. 4, no. 1, p. 1800304, 2019.